7956 *Biochemistry* **2010,** *49,* 7956–7965
DOI: 10.1021/bi101159s

BIOCHEMISTRY
including biophysical chemistry & molecular biology
Article

Recombinant Expression, in Vitro Refolding, and Biophysical Characterization of the Human Glucagon-like Peptide-1 Receptor[†]

Kathrin Schröder-Tittmann,*[,‡] Eva Bosse-Doenecke,[‡] Steffen Reedtz-Runge,[§] Christian Ihling,[∥] Andrea Sinz,[∥] Kai Tittmann,[⊥] and Rainer Rudolph[‡]

[‡]*Institute of Biochemistry and Biotechnology, Martin-Luther-University, Halle-Wittenberg, Kurt-Mothes-Strasse 3, 06120 Halle/Saale, Germany,* [§]*Department of Structure and Biophysical Chemistry, Novo Nordisk, 2760 Maløv, Denmark,* [∥]*Department of Pharmaceutical Chemistry and Bioanalytics, Institute of Pharmacy, Martin-Luther-University, Halle-Wittenberg, Wolfgang-Langenbeck-Strasse 4, 06120 Halle/Saale, Germany, and* [⊥]*Albrecht-von-Haller-Institute and Göttingen Center for Molecular Biosciences, Georg-August-University Göttingen, Ernst-Caspari-Haus, Justus-von-Liebig-Weg 11, 37077 Göttingen, Germany*

Received July 21, 2010; Revised Manuscript Received August 5, 2010

ABSTRACT: Activation of the glucagon-like peptide-1 receptor (GLP-1R) upon ligand binding leads to the release of insulin from pancreatic cells. This strictly glucose-dependent process renders the receptor and its ligands useful in the treatment of type II diabetes mellitus. To enable a biophysical characterization in vitro, we expressed the human full-length GLP-1R in the cytosol of *Escherichia coli* as inclusion bodies. After purification, refolding of the SDS-solubilized receptor was achieved by the exchange of SDS against the detergent Brij78 using an artificial chaperone system. Far-UV circular dichroism spectroscopic studies revealed that the receptor adopts a characteristic α-helical structure in Brij78 micelles. Ligand binding of the renatured protein was quantified by fluorescence quenching and surface plasmon resonance spectroscopy. In the presence of Brij micelles, the refolded receptor binds the agonist exendin-4 with an apparent dissociation constant of approximately 100 nM in a reversible one-step mechanism. To demonstrate that the detected ligand binding activity is not only due to an autonomously functional N-terminal domain (nGLP-1R) but also due to additional contacts with the juxtamembrane part, we separately expressed and refolded the extracellular domain relying on identical protocols established for the full-length GLP-1R. In support of the suggested multidomain binding mode, the nGLP-1R binds exendin-4 with a lower affinity (K_{app} in the micromolar range) and a different kinetic mechanism. The lower ligand affinity of the nGLP-1R results entirely from a decreased kinetic stability of the receptor−ligand complex, dissociation of which is ∼40-fold faster in the case of the nGLP-1R compared to the full-length GLP-1R. In summary, a framework was developed to produce functional human full-length GLP-1R by recombinant expression in *E. coli* as a prerequisite for eventual structure determination and a rigorous biophysical characterization including protein variants.

The glucagon-like peptide-1 receptor (GLP-1R)[1] was first cloned in 1992 and belongs to the group of G-protein-coupled receptors (GPCRs) (*1*), which constitute the largest and most diverse class of transmembrane proteins. The common structural features of these proteins are an extracellular N-terminal domain (Nt-domain), seven α-helical transmembrane segments connected by intracellular and extracellular loops, and an intracellular C-terminal tail. The C-terminus and several transmembrane helices are responsible for the interaction with G-proteins and other intracellular binders mediating the connection to signal cascades or initiating receptor endocytosis. GPCRs are subdivided into several families, with the GLP-1R belonging to class B (*2*). The distinctive long extracellular domain of members of class B contains three conserved disulfide bonds and is known to be essential for ligand binding. For some members of this family, high-affinity ligand binding of the isolated Nt-domain could be demonstrated in vitro after recombinant expression (*3*−*6*). GPCRs represent one of the major targets of modern drug therapy. The majority of best-selling drugs and ∼40% of all pharmaceuticals on prescription on the market address GPCRs. The native ligand of the GLP-1R, peptide hormone GLP-1, is secreted by the duodenum in response to high glucose levels, which in turn triggers the release of insulin from pancreatic cells (*7*). This ability renders GLP-1 extremely useful in the treatment of non-insulin-dependent diabetes mellitus type II (*8*). A direct application of this peptide is limited because of its rapid degradation in vivo (circulation half-life of ∼2−5 min) by the enzyme dipeptidyl-peptidase IV (DPP4) (*9*). The peptide agonist exendin-4 consists of 39 amino acids and was originally isolated from the venom of the lizard *Heloderma suspectrum* (*10*). It is 50% homologous with GLP-1 and is more resistant to degradation, so that it has been approved for therapeutic application as Exenatide.

The structures of the antagonist- and agonist-bound isolated Nt-domain (nGLP-1R) were recently reported by Runge et al. (*11*, *12*) and provide insights into the binding

[†]This work was supported by the Deutsche Forschungsgemeinschaft (Sonderforschungsbereich 610).

*To whom correspondence should be addressed. E-mail: kathrin.schroeder@biochemtech.uni-halle.de. Telephone: ++49-345-5524861. Fax: ++49-345-5527013.

[1]Abbreviations: GLP-1, glucagon-like peptide-1; GLP-1R, glucagon-like peptide-1 receptor; GPCRs, G-protein-coupled receptors; nGLP-1R, N-terminal domain of the human GLP-1 receptor; PTH, parathyroid hormone; SDS, sodium dodecyl sulfate; SRP, surface plasmon resonance.

 Published on Web 08/06/2010

mode of GLP-1 and exendin-4 (9−39) on a molecular level. Further structural information for ligand-bound Nt-domains of class B GPCRs is available for mouse CRF (corticotropin releasing factor) receptor 2β (*13*), the human PACAP (pituitary adenylate cyclase activating polypeptide) receptor (*14*), the human PTH (parathyroid hormone) receptor (*15*), and the human GIP (gastric inhibitory polypeptide) receptor (*6*). As ligand binding and signal transduction also involve juxtamembrane regions of class B GPCRs, these results show only part of the receptor activation process. In the case of the GLP-1R, structural data revealed that C-terminal part of ligand GLP-1 binds to the Nt-domain, whereas the N-terminal part of GLP-1 is expected to bind to the juxtamembrane region. Thus far, three-dimensional structures of full-length class B receptors are not available but eagerly awaited. To obtain sufficient quantities of full-length GPCRs for biophysical characterization as well as structure determination, different expression systems have been employed, including *Escherichia coli* (*16*), *Pichia pastoris* (*17*), and Sf9 insect cells (*18*). So far, few data addressing the biophysical properties of GPCRs are available in the literature (*19*−*22*). Except for rhodopsin (*23*), all published structures of GPCRs were determined after heterologous expression of genetically engineered variants in Sf9 insect cells, namely, human β_2-adrenergic receptors 1 (*24*) and 2 (*18*) and the human A_{2A} adenosine receptor (*25*).

Herein, we report on the biophysical and functional characterization of the human glucagon-like peptide-1 receptor recombinantly expressed in *E. coli*. This system combines comparatively high expression yields with the accumulation of protein in the insoluble inclusion bodies, which prevents toxic effects associated with membrane addressing. After successful purification and refolding of the receptor using a modified artificial chaperone system (*26*), we employed fluorescence spectroscopy and surface plasmon resonance to analyze ligand binding in the presence of micelles. For structural characterization, far-UV circular dichroism spectra were analyzed. To exclude the fact that the observed ligand binding reflects the autonomous functionality of the receptor Nt-domain, we separately expressed, refolded, and characterized this domain, relying on the established protocols for the full-length receptor. Results from binding experiments were compared with those obtained for the full-length receptor under standardized conditions for both proteins.

MATERIALS AND METHODS

Reagents and E. coli Strains. Restriction enzymes were obtained from New England Biolabs. *E. coli* strains Top10 and BL21(DE3)c$^+$ RIL were obtained from Novagen. Yeast extract for fed-batch fermentation was purchased from Deutsche Hefewerke GmbH and Co. (Hamburg, Germany). All other chemicals were obtained from VWR International GmbH, Sigma-Aldrich Chemie GmbH, Carl Roth GmbH, and AppliChem GmbH. Quartz doubly distilled water was used throughout the experiments. All kits for molecular biology were purchased from QIAGEN GmbH (Hilden, Germany).

Determination of Protein Concentrations. The concentrations of the full-length GLP-1R and nGLP-1R were determined spectrophotometrically at 280 nm using calculated molecular absorption coefficients of 124.570 M^{-1} cm^{-1} (full-length GLP-1R) and 46.325 M^{-1} cm^{-1} (nGLP-1R), respectively.

Construction of the Expression Plasmid. The cDNA encoding the full-length GLP-1 receptor was optimized for bacterial (*E. coli*) expression and synthesized by GENEART AG (Regensburg, Germany). The synthetic DNA was inserted into pET28a using *Nde*I and *Hin*dIII restriction sites and transformed into *E. coli* strain Top 10. The plasmid DNA of the clones was isolated using the QIAprep Spin Miniprep Kit. DNA sequence identity was confirmed by sequencing (Eurofins MWG Operon). The resulting expression vector pET28a-GLP-1R encoded an N-terminal six-His tag followed by a thrombin cleavage site and the GLP-1R.

The detailed cDNA sequence can be provided on request. Construction of the expression vector for the nGLP-1R was previously described (*27*).

Expression of GLP-1R Constructs in a Bioreactor. *E. coli* strain BL21(DE3)c$^+$ RIL was transfected with expression vectors encoding the different targets, and approximately 10 colonies were transferred to 200 mL LB precultures. The overnight preculture was inoculated into a 10 L bioreactor (BIOSTAT C-DCU, Sartorius Stedim) and grown exponentially in a 6 L fed-batch process in full medium (50 g/L yeast extract, 0.5 g/L ammonium chloride, 5 g/L glucose, 11 g/L dipotassium hydrogen phosphate, and 0.68 g/L magnesium sulfate) containing the appropriate antibiotics at 37 °C and at a constant pH of 7.0. During the fermentation process, stirring and air supply were permanently controlled and adjusted to maintain a constant partial pressure of oxygen of 30%. After complete consumption of glucose, a feeding solution (30 g/L yeast extract and 125 g/L glucose) was added with a feeding rate of approximately 4 mL/min. At an OD_{600} of ∼40−50, protein expression was induced by addition of 1 mM IPTG. In the case of full-length receptor expression, induction was conducted at 42 °C. The N-terminal domain was expressed at 37 °C. After 4 h, cells were harvested by centrifugation and pellets were stored at −20 °C.

Inclusion Body Isolation of the Full-Length Receptor and nGLP-1R. The cell pellet (250 g) was resuspended in 800 mL of 100 mM Tris-HCl (pH 7.0) and 1 mM ethylenediaminetetraacetic acid (EDTA) and, after treatment, with lysozyme (1.5 mg/g of cells, for 60 min at room temperature) and lysed by high-pressure homogenization. To digest nucleic acids, DNase was added (10 μg/mL solution) and the mixture incubated for 60 min at 4 °C. Inclusion bodies (ibs) were recovered by centrifugation (35000*g* for 30 min) at 4 °C, washed with 100 mM Tris-HCl (pH 7.0), 1 mM EDTA, and 1% Triton X-100, and centrifuged again. After being repeatedly washed with buffer containing 100 mM Tris-HCl (pH 7.0), 20 mM EDTA, 1 M sodium chloride, and, finally, 100 mM Tris-HCl (pH 7.0) and 1 mM EDTA, ibs were stored at −20 °C. Solubilization of ibs was achieved in 100 mM Tris-HCl (pH 8.0), 100 mM DTT, 20 mM SDS, and 1 mM EDTA to a final concentration of 10 μg of ibs/mL of buffer. Before purification, the solubilized receptor was exhaustively dialyzed against a buffer containing 50 mM sodium phosphate (pH 4.5) and 10 mM SDS and cleared from insoluble material by centrifugation (48000*g* for 30 min) at 20 °C. Cell lysis and isolation of the inclusion bodies of the shortened variant were performed as described by Rudolph et al. (*28*).

Purification and Renaturation of the Solubilized GLP-1R. The solutions containing the solubilized GLP-1 receptor

were adjusted to pH 8.0, subsequently loaded onto a Ni^{2+}-NTA matrix (flow rate of 0.5 mL/min), and washed with 3 column volumes of 50 mM sodium phosphate (pH 8.0) and 10 mM SDS at a flow rate of 2 mL/min. For protein elution, a buffer containing 50 mM sodium phosphate (pH 4.5) and 10 mM SDS was applied to the column.

Protein pulse renaturation was conducted at room temperature. Three pulses of a purified protein solution (0.03 mg/mL protein per pulse in the refolding mixture) were sequentially injected in intervals of at least 6 h into a refolding buffer containing 100 mM Tris-HCl (pH 8.5), 1 M L-arginine, 1 mM EDTA, 20 mM β-methylcyclodextrin, 5 mM GSH, 1 mM GSSG, and 3 mM Brij78. The stirrer speed was set to 200 rpm for 10 min. After incubation for 36 h, the solution was centrifuged at 48000*g* for 60 min at 4 °C, dialyzed against a buffer with 50 mM sodium phosphate (pH 7.4), 150 mM sodium chloride, 0.5 mM Brij78, 1 mM GSH, and 0.2 mM GSSG, and subjected to another centrifugation. The clear supernatant was applied to Amicon concentrators (50 kDa molecular mass cutoff) and concentrated by ultrafiltration until protein concentrations of approximately 0.4 mg/mL protein were achieved.

Spectroscopic Analysis by Far-UV Circular Dichroism (CD) and Fluorescence Spectroscopy. Far-UV CD spectra of GLP-1R were recorded using a JASCO J-810 spectropolarimeter in a 1 mm quartz cuvette at 20 °C. Spectra of the native protein were recorded in 50 mM sodium phosphate (pH 7.4) and 0.1 mM Brij78 and those of the SDS-solubilized receptor sample in 50 mM sodium phosphate (pH 7.4) and 10 mM SDS. Spectra of denatured protein samples were recorded after dialysis of the native protein against buffer containing 50 mM sodium phosphate (pH 7.4), 6 M denaturant guanidine hydrochloride, and 0.1 mM Brij78. Data were collected at a scanning rate of 50 nm/min with a bandwidth of 1 nm and a response time of 2 s. The scanning range was adjusted to 260−190 nm. The spectra were 60-fold accumulated and averaged, corrected for buffer contributions, and converted to mean residue ellipticity according to the method of Schmid (*29*) using a calculated molecular mass (M_r) of 53126.5 Da. The secondary structure contents were estimated using CDNN (*30*).

Fluorescence emission spectra were recorded at 20 °C on a FluoroMax-3 (JOBIN YVON) fluorescence spectrometer in a 10 mm quartz cuvette. The excitation wavelength was set to 295 nm, and emission spectra were recorded between 310 and 400 nm. The slit widths were set to 5 nm. The protein concentration of the GLP-1R was adjusted to 0.5 μM in 50 mM sodium phosphate (pH 7.4), 150 mM sodium chloride, and 0.1 mM Brij78. Spectra of denatured protein samples were recorded after dialysis of the native receptor against 50 mM sodium phosphate (pH 7.4) supplemented with 6 M guanidine hydrochloride. For analysis of receptor−ligand complexes, samples containing equimolar concentrations of the receptor and ligand were prepared. Spectra were recorded after preincubation for 3 min. All spectra were corrected for buffer contributions.

Determination of Ligand Binding Constants Using Surface Plasmon Resonance (Biacore). To biophysically characterize ligand binding of the refolded full-length GLP-1R and nGLP-1R, surface plasmon resonance measurements using a Biacore T100-System were conducted. Cysteinylated GLP-1, exendin-4, and parathyroid hormone (PTH, negative control) were immobilized on a CM 5 chip using NHS/EDC activation and disulfide coupling with an immobilization level of 100−600 response units. Binding experiments were performed in running buffer containing 50 mM sodium phosphate (pH 7.4), 150 mM sodium chloride, and 0.1 mM Brij78. The chip was regenerated by treatment with a solution containing 6 M urea. Unspecific binding was monitored on an additional surface that was blocked with cysteine. All sensorgrams were corrected for unspecific binding. Before injection, protein samples were dialyzed against running buffer and injected at a flow rate of 30 μL/min. For analysis, binding curves were fitted using T100 BIAevaluation (Biacore AB, Uppsala, Sweden) according to the 1:1 Langmuir binding model or, when necessary, more complex (multistep) models.

In competition experiments, a preincubation of the receptor with ligands was conducted with varied concentrations of GLP-1 or exendin-4 for 30 min at room temperature. The mixture was subsequently injected onto the sensor chip surface at a flow rate of 30 μL/min. Calculation of the dissociation constant was performed using eqs 1 and 2.

$$S_{GGW} = S_{GGW}{}^0 - \Delta S_{max}\frac{[R-L]}{[R_0]} \quad (1)$$

where S_{GGW} is the measured resonance signal of the receptor−ligand complex after injection under equilibrium conditions, $S_{GGW}{}^0$ is the resonance signal of the receptor−ligand complex after injection under equilibrium conditions without preincubation of the receptor with ligand (competitor), ΔS_{max} is the resonance signal at maximum saturation of receptor with ligand, [R−L] is the concentration of the receptor−ligand complex, and [R_0] is the total concentration of the receptor. According to the law of conservation of mass, the concentration of the receptor−ligand complex can be calculated with a quadratic function that is substituted into eq 1:

$$S_{GGW} = S_{GGW}{}^0 - \frac{\Delta S_{max}}{2[R_0]}\left[[L_0]+[R_0]+K_D - \sqrt{([L_0]+[R_0]+K_D)^2 - 4[L_0][R_0]}\right] \quad (2)$$

where [L_0] is the concentration of free ligand and K_D is the ligand dissociation constant.

Determination of Ligand Dissociation Constants by Fluorescence Quenching Experiments. In addition to the surface plasmon resonance experiments, the ligand binding of GLP-1R was quantitatively analyzed by fluorescence spectroscopy relying on the quenching of the intrinsic receptor fluorescence by sequential titration with exendin-4 and formation of a receptor−ligand complex. Tryptophan fluorescence emission spectra of GLP-1R were recorded between 335 and 355 nm after excitation at 295 nm on a FluoroMax-3 (JOBIN YVON) fluorescence spectrometer using a 10 mm quartz cuvette at 20 °C. Beforehand, the cuvette was equilibrated overnight at room temperature with a receptor solution to ensure a stable signal. Emission spectra were recorded 2 min after addition of ligand and continuous stirring of the solution. For data analysis, fluorescence intensities at 342 nm were deployed. All spectra were corrected for buffer contributions. Calculation of the dissociation constant was performed using a quadratic function (eq 3).

$$F = F_0 - \frac{\Delta F_{max}}{2[R_0]}\left[[L_0]+[R_0]+K_D - \sqrt{([L_0]+[R_0]+K_D)^2 - 4[L_0][R_0]}\right] + F_{Lig}[L_0] \quad (3)$$

where F is the measured total fluorescence, F_0 is the intrinsic fluorescence of the receptor, ΔF_{max} is the maximum change in fluorescence at total saturation of receptor with ligand, $[R_0]$ and $[F_0]$ are the total concentrations of receptor and ligand, respectively, K_D is the dissociation constant, and F_{Lig} reflects the intrinsic concentration-dependent fluorescence signal of the ligand. F_{Lig} was determined in independent experiments, in which exendin-4 was sequentially titrated into buffer in the absence of the GLP-1R. Data were quantitatively analyzed assuming that the intrinsic fluorescence of the ligand is not affected by binding to the receptor.

Reversed-Phase HPLC. The homogeneity of native and denatured protein samples was analyzed by reversed-phase HPLC deploying an analytical EC 125/4 NUCLEOSIL 500−5 C3 PPN reversed-phase column from Macherey&Nagel GmbH and Co. Chromatographic analysis was performed at room temperature applying solvent B linear gradients from 1 to 25% (15 min), 25 to 55% (60 min), and 75 to 90% (15 min) (solvent A being 0.1% TFA in water and solvent B being 80% acetonitrile and 0.1% TFA in water).

Disulfide Pattern Analysis by LC−MS. HPLC fractions were dried under vacuum and resuspended in 100 μL of buffer containing 100 mM Tris-HCl (pH 7.8) and 10 mM $CaCl_2$. Subsequently, 4 μg of chymotrypsin was added, and proteolytic digestion of GLP-1R was conducted at 37 °C for 16 h. Peptide mixtures from enzymatic digests were analyzed by *offline* nano-HPLC/MALDI-TOF/TOF mass spectrometry. Peptides were separated by reversed-phase chromatography on an Ultimate 3000 nano-HPLC system (Dionex Corp., Idstein, Gemany) with PepMap C18 columns [precolumn, 300 μm × 5 mm, 5 μm, 100 Å; separation column, 75 μm × 150 mm, 3 μm, 100 Å (Dionex Corp.)]. After the peptides had been washed on the precolumn for 15 min with water containing 0.1% TFA, they were eluted and separated with linear gradients from 5 to 35% B (90 min), 35 to 100% B (1 min), and 100% B (5 min), where solvent A was 5% acetonitrile containing 0.05% TFA and solvent B was 80% acetonitrile containing 0.04% TFA. The eluates were fractionated postcolumn onto a 384 MTP 800 μm Anchor Chip MALDI target (Bruker Daltonik, Bremen, Germany) using an LC/MALDI fraction collector (Proteineer FC, Bruker Daltonik) and cocrystallized with α-cyano-4-hydroxycinnamic acid (CHCA) as a matrix. Mass spectra were automatically acquired using an Ultraflex III MALDI-TOF/TOF instrument (Bruker Daltonik) in the positive ionization and reflectron mode. Per target spot, a total of 2000 laser shots were automatically acquired and added to a spectrum in the m/z range of 800−5000. Detected peptide signals with a signal-to-noise ratio of >10 were automatically subjected to MALDI-LIFT-TOF/TOF-MS/MS to acquire fragment ion mass spectra of the respective peptides. Data acquisition and data processing were performed with Flex Control version 3.0 and Flex Analysis version 3.0 that were controlled by WarpLC 1.1 (Bruker Daltonik).

Identification of Disulfides by MS. Putative disulfide-linked peptides were identified on the basis of their experimental mass (maximum tolerance of 30 ppm) using GPMAW (General Protein Mass Analysis for Windows) version 8.0 (Lighthouse Data, Odense, Denmark) and BioTools 3.1 (Bruker Daltonik). MS/MS data are required for confirmation of peptide disulfides. As disulfide-linked peptides usually yield poor quality fragment spectra, we used the phenomenon of in-source reduction of disulfides during MALDI and employed MS/MS data of the single peptides containing reduced cysteines for confirmation of the peptide disulfides (*31*, *32*). BioTools was used to assign m/z values of peptides in the fragment ion mass spectra with a mass tolerance of 0.8 unit.

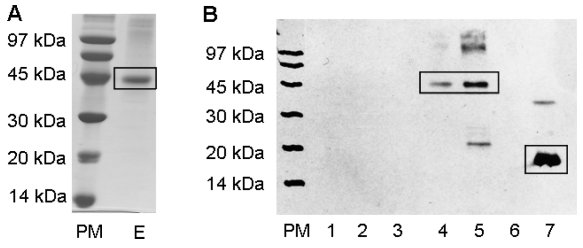

FIGURE 1: SDS−PAGE (A) and Western blotting (B) analysis of GLP-1R purification. (A) PM denotes molecular mass markers and E the elution fraction of Ni-NTA affinity chromatography. (B) Western blotting with a specific antibody against the N-terminal domain of the GLP-1R. PM denotes the molecular mass marker. Lane 1: protein pattern prior to induction. Lane 2: after induction for 2 h. Lane 3: after induction for 4 h. Lane 4: SDS-solubilized inclusion body proteins. Lane 5: GLP-1R after purification on Ni-NTA. Lane 6: negative control (recombinantly expressed, purified GIP receptor). Lane 7: positive control (nGLP-1R). Bands of purified receptor proteins are boxed.

RESULTS

Expression and Refolding of the Full-Length GLP-1 Receptor. The N-terminal extracellular domain of the GLP-1 receptor (nGLP-1R) was previously shown to play an important role in ligand binding and selectivity (*27*). Recombinant expression and refolding of this fragment provided sufficient amounts of protein for crystallization and structure determination by X-ray crystallography (*11*, *12*). For a characterization of the full-length GLP-1R reyling on the same strategy, a codon usage optimization of the receptor-encoding DNA for recombinant expression in *E. coli* was indispensable because expression trials using wild-type cDNA did not lead to detectable yields of the receptor under all conditions tested, including different sets of vectors and fusion constructs (data not shown). The first 23 amino acids of GLP-1R consist of a signal sequence that is not present in the mature protein. Arg24 is thus predicted to be the N-terminal amino acid residue of the in vivo processed receptor.

A synthetic, codon-optimized GLP-1R cDNA was expressed in *E. coli* as insoluble aggregates (inclusion bodies). As a first purification step, preparation of inclusion bodies after cell disruption was conducted. At this stage of purification, the receptor protein could not be detected by SDS−PAGE analysis but by Western blotting applying an antibody against the N-terminal domain of the GLP-1R (Figure 1). For an efficient solubilization of the isolated inclusion bodies, strongly denaturing and reducing conditions had to be employed via addition of 100 mM DTT and 20 mM SDS to the solubilization buffer. For final purification of the N-terminally His-tagged protein, Ni-NTA-based affinity chromatography was used. The homogeneity of the protein was ~95% as estimated by SDS−PAGE analysis (Figure 1). The total yield of pure protein per liter of cell culture amounted to ~70−80 mg before pulse renaturation.

To obtain native protein, we established a refolding protocol. During renaturation, the ionic detergent SDS was complexed by the addition of β-methylcyclodextrin. Stabilization of the transmembrane helices was ensured by the addition of the mild detergent Brij78. To provide optimal conditions for disulfide bond formation, a redox shuffling system consisting of GSH and GSSG was included in the renaturation buffer. Furthermore, the

presence of high molar concentrations of L-arginine turned out to be essential for refolding of the GLP-1R. After renaturation, aggregates were removed by centrifugation. The yield of the soluble receptor after pulse renaturation amounted to ~50−80%. On the basis of quantitative analysis of ligand binding by fluorescence quenching, the amount of functionally refolded receptor was estimated to be > 85% of the amount of the soluble receptor (see below).

The identity of the GLP-1R after purification and refolding was confirmed by the use of a specific antibody against the N-terminal domain of the receptor (Figure 1) and MALDI mass spectrometry of a trypsin-digested receptor sample (data not shown).

Secondary and Tertiary Structure Analysis of the Recombinant GLP-1 Receptor. To gather information about the structure of the refolded receptor, secondary structure elements were analyzed by far-UV CD spectroscopy under native and denaturing conditions (Figure 2). The far-UV CD spectrum of the receptor under nativelike conditions (Brij micelles) as well as in SDS micelles clearly indicates a high content of secondary structure elements. Unfolded segments, which would provide a very strong negative contribution around 190 nm in the CD spectrum, are clearly absent for the refolded receptor. Using CDNN (*30*), we estimated a higher α-helical content for the native protein (~40%) than for the SDS-solubilized receptor (~25%). This observation suggests that the transmembrane segments of native GLP-1R, which amount to ~35% of the protein, fold into helices. The CD spectrum of the GLP-1R in guanidine hydrochloride is limited to wavelengths of > 210 nm because of the strong absorbance of the denaturant. As expected, the spectrum clearly indicates a small content of residual secondary structure elements.

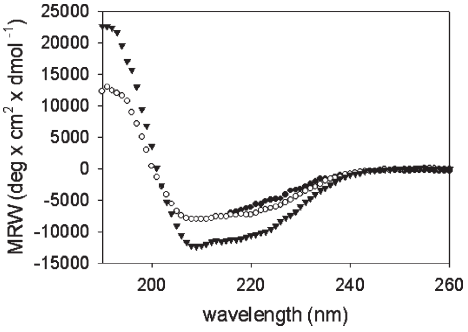

FIGURE 2: Far-UV CD spectra of native and the chemically denatured full-length GLP-1R. The spectrum of native protein (▼) was recorded in 50 mM sodium phosphate (pH 7.4) and 0.1 mM Brij78. Spectra of SDS-treated or unfolded protein were recorded either in 50 mM sodium phosphate (pH 7.4) and 10 mM SDS (○) or after dialysis of the native protein against buffer containing 50 mM sodium phosphate (pH 7.4), 6 M guanidine hydrochloride, and 0.1 mM Brij78 (●). Full conditions are detailed in Materials and Methods.

In addition, the intrinsic tryptophan fluorescence of the GLP-1R was analyzed by steady-state fluorescence spectroscopy. While refolded GLP-1R exhibited an emission maximum at 341 nm, the guanidine-denatured sample emits with a red shift of 10 nm at 351 nm (Figure 1 of the Supporting Information).

Ligand Binding Properties of the Recombinantly Expressed Full-Length GLP-1 Receptor. To evaluate functionality, i.e., ligand binding competence of the refolded receptor, we first conducted steady-state fluorescence measurements of samples containing the GLP-1R and ligand in a 1:1 molar (equimolar) ratio. For an evaluation of the spectroscopic effect upon ligand binding, we compared the measured spectrum of the putative GLP-1R−ligand complex with a theoretical spectrum obtained by addition of spectra of the free receptor and free ligand. In this approach, addition of both peptide ligands, GLP-1 and exendin-4, to the GLP-1R induced a bathochromic shift of the tryptophan fluorescence emission maximum of ~3 nm and a quench of fluorescence intensity (Figure 3A,B). As a negative control, addition

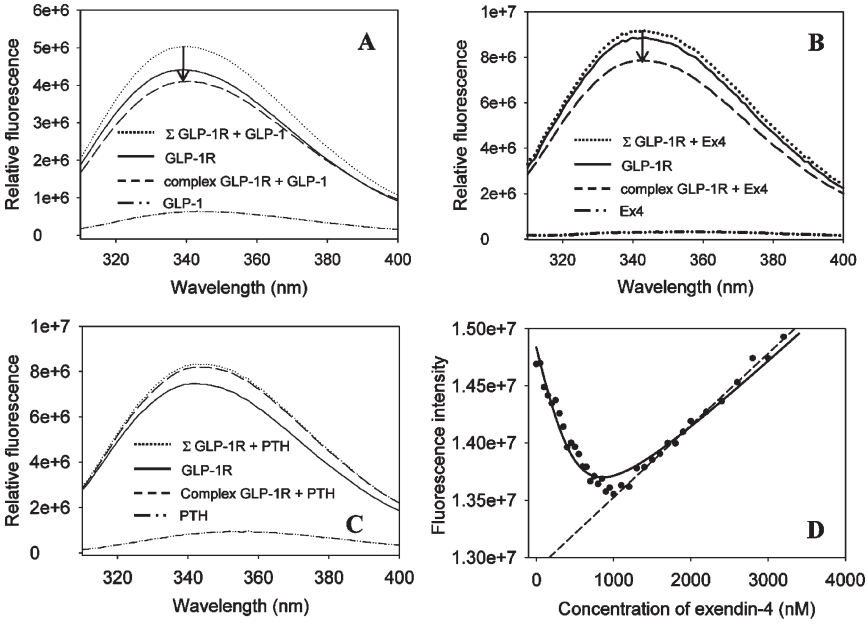

FIGURE 3: Fluorescence spectra of the free and ligand-bound GLP-1R and titration of the GLP-1R with exendin-4. The solid lines in panels A−C represent the spectra of the free GLP-1R, the dashed lines the experimentally derived spectra of the GLP-1R in the presence of an equimolar amount of ligand, and the dotted lines the spectra of the theoretical sum calculated from the spectra of the free receptor and free ligand. The dashed and dotted lines show spectra of ligands GLP-1 (A), exendin-4 (B), and PTH (C). The concentrations of the receptor and coresponding ligand were either 150 (A) or 200 nM (B and C). (D) Fluorescence signal at 342 nm during titration of 500 nM GLP-1R with exendin-4. Evaluation of the dissociation constant from the fluorescence signals using eq 3 yielded a K_D of 116 ± 18 nM. The dashed line (linear regression fit) corresponds to the linear increase in the intrinsic concentration-dependent fluorescence signal of the ligand.

Table 1: Ligand Binding Constants of the Full-Length GLP-1R versus the nGLP-1R

	full-length GLP-1R	nGLP-1R
K_D^{app} for exendin-4 (nM)	116 ± 18 (fluorescence quenching) 103 ± 9 (SRP, saturation binding) 180 ± 60 (SRP, competition)	950 ± 140 (SRP, saturation binding)
kinetic stability of the receptor−exendin complex ($t_{1/2}$) (s)	800	15−20
kinetic model of binding	one-step reversible	multistep reversible

of PTH, a hormone peptide ligand of another class B GPCR, did not lead to any change of the emission maximum of the GLP-1 receptor (Figure 3C). These date indicate a specific interaction of GLP-1 and exendin-4 with the recombinantly produced and refolded GLP-1 receptor.

To determine the ligand dissociation constant of the refolded GLP-1R, fluorescence titration experiments were conducted. Exendin-4 was sequentially added to a sample containing 500 nM receptor, and fluorescence emission spectra were recorded 2 min after mixing. Addition of exendin-4 initially caused a quenching of the overall fluorescence signal monitored at 342 nm (Figure 3D). At the stage of complete saturation of the receptor with ligand, a linear increase in the magnitude of the signal caused by the intrinsic fluorescence of exendin-4 was observed. Evaluation of the measured data by a quadratic function resulted in a dissociation constant of 116 ± 18 nM ($p < 0.0001$) (Figure 3D and Table 1). To estimate the fraction of the functionally refolded receptor, we were fitting the data by assuming different fractions of functional receptor starting with 500 nM (100% yield) and sequentially decreased the "functional fraction" stepwise in 5% steps. Our analysis clearly revealed that the corresponding fits cannot accommodate the data when a fraction of ≤85% functional protein is assumed, whereas small differences in the concentration (90% functional protein) are tolerated, yielding comparable K_D values. In the case of GLP-1, the intensity of GLP-1R fluorescence quenching was too small upon ligand titration (compare Figure 3A) to allow a reliable estimation of a dissociation constant by this method (data not shown).

As a second and independent method for analyzing the ligand binding properties of the full-length GLP-1R in a quantitative manner, surface plasmon resonance measurements were conducted. Modified ligand peptides containing a linker sequence followed by an additional cysteine at the C-terminus were employed. The additional cysteine permitted attachment of the ligands to the sensor chip surface via disulfide coupling without interfering with its binding capability. As a negative control, unspecific binding of refolded GLP-1R to the sensor surface with immobilized PTH (ligand of the related class B GPCR PTH receptor) was not observed.

Upon injection of the GLP-1R onto the surface coated with exendin-4, binding was observed in a concentration-dependent manner (Figure 4A). Quantitative analysis of these binding studies with Biacore T100 Evaluation according to a reversible one-step mechanism revealed an on rate constant k_{on} of (8.51 ± 0.14) × 10^3 M^{-1} s^{-1} and a dissociation rate constant k_{off} of (8.44 ± 0.12) × 10^{-4} s^{-1} to give a K_D value (k_{off}/k_{on}) of 99 nM for exendin-4 (Table 1). Similar dissociation constants of the GLP-1R for exendin-4 could be estimated with independent batches of the GLP-1R and gave a K_D of 103 ± 9 nM ($n = 3$). In similar experiments, binding of the native ligand GLP-1 by the GLP-1R was detectable (data not shown). However, because of poor response signals (~5 resonance units) caused by formation of a GLP-1R−GLP-1 complex, no dissociation constant could be reliably estimated in this type of experiment. Remarkably, binding of GLP-1 to the isolated N-terminal domain can be reliably analyzed by SPR [800 resonance units, identical to the chip that was used for the full-length GLP-1R (see Figure 3 of the Supporting Information)], indicating a different ligand binding mode in the full-length receptor and the N-terminal domain.

In a complementary approach, competition experiments on the exendin-4 sensor chip were conducted by preincubation of GLP-1R with increasing concentrations of exendin-4. As expected, a decrease in maximum resonance signal values with increasing competitor concentrations could be monitored (Figure 4C). Data analysis was conducted by nonlinear regression (eq 2), resulting in a dissociation constant of 180 ± 60 nM ($p = 0.04$) (Figure 4D). Because of the small response signals observed for Biacore binding analysis of GLP-1 (see above), no competition experiments were performed with the latter ligand. Taken together, these results show that the recombinantly produced and refolded full-length GLP-1 receptor binds to its ligands in a specific manner with a dissociation constant for exendin-4 in the nanomolar range.

Characterization of the N-Terminal Domain of the GLP-1R. It has been shown previously that the isolated N-terminal domain of GLP-1R exhibits specific binding with high affinity for its ligands and further possesses a distinct disulfide pattern (*5*). To verify that the observed ligand binding of refolded GLP-1R samples is not simply due to an autonomous functionality of the N-terminal domain, we purified and refolded the nGLP-1R exactly as the full-length protein and investigated its binding behavior under conditions identical to those of the full-length receptor in presence of Brij micelles. Another important point was to validate that the disulfide bridges within the nGLP-1R can be formed correctly under the refolding conditions established for the full-length receptor. The fragment encoding the 125 N-terminal amino acids of the GLP-1R without the putative signal sequence was recombinantly expressed in *E. coli*, and inclusion bodies were isolated as described by Rudolph et al. (*28*). Purification and refolding were conducted using the protocols for the full-length GLP-1R and resulted in a homogeneous species of the protein sample (data not shown). MALDI mass spectrometry confirmed the correct mass of 16468 Da of the refolded receptor fragment (data not shown). The homogeneity of disulfide bonding of the purified and refolded protein was confirmed by reversed-phase HPLC and compared to that of a sample that was purified and refolded as described by Bazarsuren et al. (*5*). Both protein samples feature the same elution behavior (Figure 2 of the Supporting Information), indicating a correct disulfide bond formation. To further prove correct refolding of the N-terminal domain after renaturation using the protocol for the full-length receptor, we determined the disulfide pattern. For this purpose, an elution fraction of the refolded nGLP-1R via RP-HPLC was digested with chymotrypsin and the resulting fragments were analyzed by *offline* nano-HPLC/MALDI-TOF/TOF mass spectrometry. The determined disulfide bridges were

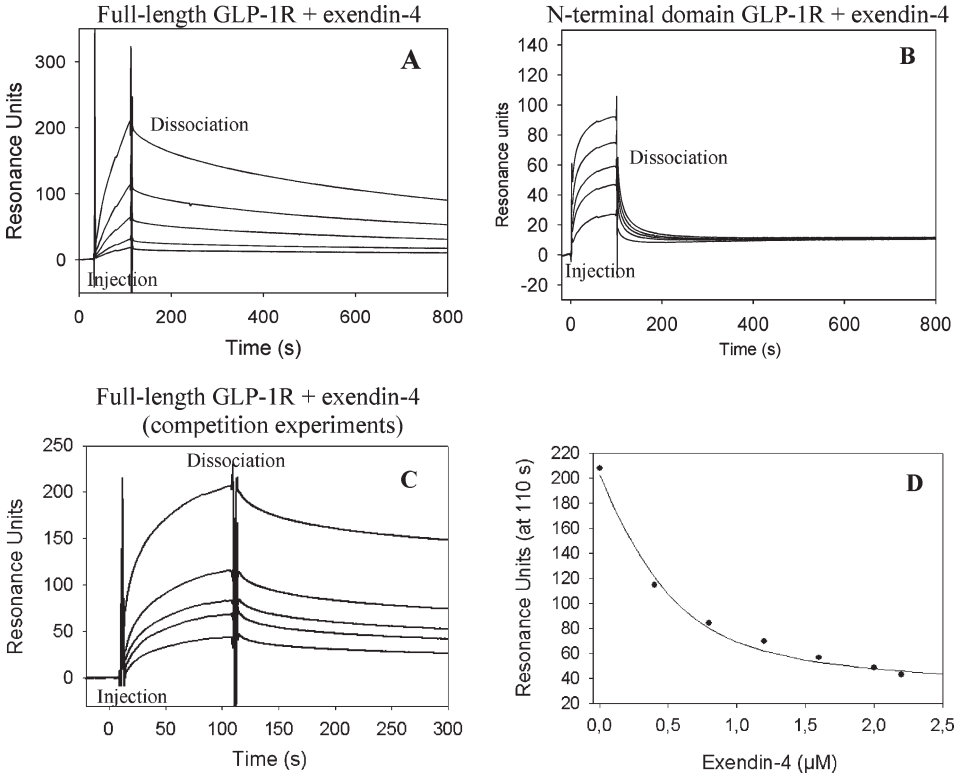

FIGURE 4: Ligand binding assays of the refolded full-length GLP-1R and nGLP-1R with exendin-4 by surface plasmon resonance. One hundred fifty resonance units of exendin-4 was covalently coupled to a Biacore CM5 sensor chip. (A) Sensorgram of the binding of (from bottom to top) 0.11, 0.45, 0.9, 1.8, and 3.6 μM GLP-1R in buffer containing 50 mM sodium phosphate (pH 7.4), 150 mM sodium chloride, and 0.1 mM Brij78 at a flow rate of 30 μL/min and 20 °C to the chip. The dissociation constant using Biacore T100 Evaluation and a 1:1 Langmuir model was estimated to be 99 nM. (B) Sensorgrams of the binding of (from bottom to top) 0.17, 0.68, 1.35, 2.7, and 5.4 μM nGLP-1R in buffer containing 50 mM sodium phosphate (pH 7.4), 150 mM sodium chloride, and 0.1 mM Brij78. Data points resulting from binding of the nGLP-1R to the ligands were fitted with Biacore T100 Evaluation and resulted in a dissociation constant of 1.0 μM for exendin-4. (C) In a competition experiment, 0.5 μM GLP-1R was preincubated with increasing concentrations of exendin-4 for 30 min at room temperature and injected onto a CM5 chip with immobilized exendin-4 (peptide concentrations from top to bottom of 0, 0.4, 0.8, 1.2, and 2.0 μM). (D) Measured plateau values with respect to competitor concentration are shown. The dissociation constant determined in the competition experiment was 180 ± 60 nM.

identical to those identified by Bazasuren. These results strongly indicate that the refolding protocol established for the full-length GLP-1R yields a correctly folded N-terminal domain of the receptor. The specific ligand binding properties of nGLP-1R were characterized by surface plasmon resonance studies. A concentration-dependent binding of both exendin-4 (Figure 4B) and GLP-1 (Figure 3 of the Supporting Information) could be observed. A marked difference in the ligand binding of the nGLP-1R versus the full-length GLP-1R is displayed in the different association and dissociation rates of the ligand−receptor complexes. Ligand binding to the nGLP-1R is slightly faster than that to the full-length receptor. In contrast, dissociation of the ligand−receptor complex is markedly slower for the full-length protein. Whereas dissociation of exendin-4 from the full-length GLP-1R has a half-time of ~800 s (see Figure 4A), GLP-1 and exendin-4 completely dissociate from the N-terminal domain within 100 s with half-times of 15−20 s (Figure 4B and Figure 3 of the Supporting Information). The binding curves with both ligands were evaluated with Biacore T100 Evaluation. This analysis revealed that binding of both ligands cannot be reliably fitted according to a simple reversible one-step model but rather require more complex models (data not shown) implying a different kinetic binding mechanism when compared to that of the full-length receptor for which a 1:1 binding model adequately described the data. The dissocation constants of both ligands were estimated thermodynamically, solely relying on the response signal under equilibrium conditions (~90 s after injection) without specifying a kinetic binding model. K_D values of 1.1 ± 0.1 μM (GLP-1) and 1.0 ± 0.1 μM (exendin-4) were derived after the data had been fit according to a steady-state affinity model using Biacore T100 evaluation. Similar dissociation constants of the nGLP-1R for both ligands could be estimated with independent batches of the nGLP-1R and gave dissociation constants of 1.0 ± 0.1 μM (n = 2) for GLP-1 and 0.9 ± 0.1 μM (n = 2) for exendin-4. A comparsion of the ligand dissociation constants of the full-length receptor versus those of the N-terminal domain reveals that the intact protein exhibits a 10-fold higher affinity, supporting the multidomain binding model according to which both the N-terminal domain and juxtamembrane parts conjointly confer ligand binding. The weaker ligand affinity of the isolated N-terminal domain results from a 40−50-fold decreased lifetime (kinetic stability) of the receptor−ligand complex compared to that of the full-length receptor. In a negative control, injection of the nGLP-1R onto a sensor surface coupled with PTH did not lead to any observable binding. In line with these observations, via tryptophan fluorescence measurements of the nGLP-1R in the presence of equimolar amounts of GLP-1, exendin-4, or PTH in a 1:1 molar ratio, binding could be detected for GLP-1 and exendin-4 but not for PTH, buttressing the results from the surface plasmon resonance studies (data not shown).

DISCUSSION

The glucagon-like peptide-1 receptor belongs to class B of the G-protein-coupled receptors and plays an important role in

glucose homeostasis. Although a rigorous biophysical characterization, analysis of ligand binding, and crystal structure determination of the isolated N-terminal domain were accomplished only recently (*5*, *11*, *12*, *27*, *33*, *34*), detailed studies addressing the full-length receptor are still lacking. The recombinant expression, purification, and (if necessary) refolding of full-length membrane proteins (MPs) into a native and functional form represents a substantial challenge that has been met with only limited success. This is mainly due to the amphiphilic character of MPs requiring their reconstitution in special environments like micelles, liposomes, or Nanodiscs (*35*). Comprehensive biophysical as well as high-resolution structural studies clearly demand sufficient amounts of homogeneous, functional protein as has been recently shown for human β_2-adrenergic receptors 1 (*24*) and 2 (*18*) and the human A_{2A} adenosine receptor (*25*).

In this study, we used a cost-efficient alternative approach by using heterologous expression of the human full-length GLP-1 receptor in *E. coli* as insoluble aggregates. The successful application of this strategy was recently reported for other GPCRs (*16*). Because expression using the wild-type (human sequence) cDNA did not result in detectable yields of receptor, optimization of the receptor-encoding DNA for expression in the desired host was mandatory. For the initial solubilization of the isolated inclusion bodies, strongly denaturing (SDS) and reducing (DTT) conditions were chosen. Purification of the His-tagged protein was accomplished by affinity (nickel-chelating) chromatography. Typically, 70−80 mg of purified protein was produced from 1 L of bacterial culture. For a successful refolding of the GLP-1R, two critical aspects had to be taken into account: (i) the correct formation of intramolecular disulfide bridges and (ii) the exchange of the denaturing detergent SDS against a milder detergent. In the course of refolding protocol optimization, numerous detergents were tested, including *n*-dodecyl β-D-maltoside, digitonin, CHAPS, and different Brij compounds. The use of polyoxyethylene(20)-stearyl ether (Brij78) resulted in the largest amount of soluble receptor in the refolding buffer. For the correct formation of the disulfide pattern, reduced glutathione and oxidized glutathione were applied as a redox-shuffling system. A 5:1 ratio of reduced GSH to oxidized GSSG turned out to be most efficient. To ensure a quantitative dissociation of SDS from the receptor protein, β-methylcyclodextrin was added to the refolding buffer. Cyclodextrins belong to the class of cyclic oligosaccharides and are composed of six to nine glucose molecules connected by O-glycosidic bonds. The resulting cyclic structure provides a cavity of defined size in which hydrophobic molecules can be captured or complexed. This refolding strategy is therefore termed the artificial chaperone-supported renaturation and was first described by Rozema and Gellmann (*26*). In addition, L-arginine as a low-molecular mass folding enhancer was present in the refolding buffer. This agent was shown to be very effective for refolding of many proteins, including the N-terminal domains of the human GLP-1 and PTH receptor-1 (*4*) and antibody Fab fragments (*36*).

The purified and refolded GLP-1 receptor appears to be (at least partially) structured as may deduced from far-UV CD spectroscopic analysis. Deconvolution of the CD spectra of the refolded receptor yielded an α-helical content of ~40%. Similar results were obtained for the human leukotriene B4 receptor BLT1 (*19*) and the μ-opioid receptor (*22*).

Specific ligand binding properties of the refolded GLP-1R were characterized by both fluorescence quenching and surface plasmon resonance experiments for the agonist exendin-4 (1−39). The dissociation constant determined by fluorescence quenching studies was 116 ± 18 nM. The dissociation constants estimated by surface plasmon resonance were 103 ± 9 nM (saturation binding experiments) and 180 ± 60 nM (competition experiments) and are thus in fair agreement with the results from fluorescence quenching measurements. The application of surface plasmon resonance for the quantitative analysis of binding behavior of a full-length GPCR was so far only described for neurotensin receptor type 1 (*21*). To the best of our knowledge, there is no GPCR-related study reporting the quantitative analysis of ligand dissociation constants by fluorescence quenching. It has to be noted that higher affinities were reported for the membrane-bound GLP-1R when enriched from disrupted eukaryotic cells by membrane preparation (*37*, *38*). On the basis of radioactive filter assays, IC_{50} values in the low nanomolar range were estimated for both exendin-4 and GLP-1. This poses the question of whether the fully functional receptor could be produced in this study. We emphasize, however, that the different assays for quantitation of ligand binding of the GLP-1R may not be directly comparable. Whereas the commonly deployed filter assay relies on radioactively labeled, iodinated ^{125}I-labeled ligands and homologous competitive binding of nonlabeled ligands to estimate IC_{50} values as affinity constants, we used surface plasmon resonance experiments to directly assess true equilibrium constants (K_D values) and rate constants of ligand binding and dissociation. In the case of filter assay analysis, it is assumed that the iodinated radioactive tracer is bound with the same affinity as the noniodinated competitors, which is a nontrivial assumption and remains to be shown. A further difference between the filter assay and Biacore assay is that the former method may not warrant true equilibrium conditions throughout sample workup because unbound ligands are removed from the filters prior to readout. On the other hand, Biacore analysis relies on interaction of immobilized ligands and their cognate receptor, and there is no guarantee that immobilization does not affect binding. As a matter of fact, we could not use the Biacore assay to analyze the interaction between the full-length GLP-1R and immobilized GLP-1, although the free ligand binds to the receptor as judged by fluorescence spectroscopy (see Figure 3). A further striking difference between the two assays refers to the chemical environment of the receptor. In our hands, the recombinantly expressed receptor had to be refolded and reconstituted in Brij micelles, which strongly differ in their chemical composition from mammalian membranes. This suboptimal environment may cause a slightly different conformation and decreased ligand affinities of the protein. Also, in contrast to eukaryotic expression systems, *E. coli* lacks the machinery for nativelike posttranslational protein modifications. The GLP-1R contains three potential glycosylation sites within the Nt-domain and two more within the first extracellular loop. The absence of linkage to oligosaccharides can indeed lead to a decrease in the level of ligand binding as shown for other receptors such as the calcitonin receptor-like receptor (*39*). In addition, previous studies indicated that ligand affinities of GPCRs depend on the coupling to their cognate heterotrimeric G-proteins as shown for the somatostatin receptor (*40*) and the latrotoxin receptor (*41*). The apparent lower affinity of the GLP-1R for its ligands could be caused by the lack of partners for forming a high-affinity ternary complex as in the membrane environment. In addition, one has to consider that micelles may not be suitable to perfectly mimic a natural membrane environment because of their stronger curvature at the surface and the innate different lateral pressure compared to those of lipid bilayers, which could in turn affect

the conformation of the receptor. Future studies will be aimed at reconstituting the recombinantly produced GLP-1R from Brij micelles into phospholipid vesicles to accommodate the receptor in a more nativelike environment and to test whether the GLP-1R exhibits higher ligand affinities in this environment than in Brij micelles.

To verify that the monitored binding properties of the full-length GLP-1R samples are not due to only the autonomous functionality of the N-terminal domain, we investigated the binding behavior of the isolated Nt-domain after purification and refolding following exactly the procedure for the full-length receptor. Determination of the disulfide pattern indicated a correct linkage of the respective cysteine residues. Surface plasmon resonance measurements revealed a concentration-dependent binding of both GLP-1 and exendin-4 to the nGLP-1R. Remarkably, because of poor response signals, binding of GLP-1 to the full-length GLP-1R could not be analyzed depite using the same chip as in case of the nGLP-1R. Exendin-4 is bound by the nGLP-1R with an approximately 10-fold decreased affinity compared to that of the full-length receptor caused by a 40−50-fold faster dissocation of the ligand. A further difference is observed for the kinetic binding mechanism. While the saturation binding data of GLP-1R could be fitted according to a reversible one-step mechanism, the mechanism for binding of GLP-1 and exendin-4 to the nGLP-1R is more complex. In view of the apparent and statistically significant differences (Table 1) in the (i) ligand affinity, (ii) kinetic stability of the receptor−ligand complexes, (iii) kinetic binding mechanism, and (iv) ability to bind GLP-1, we are convinced that the observed ligand binding of the full-length GLP-1R does not reflect autonomous binding of the N-terminal domain. We would like to point out, however, that the affinities of the nGLP-1R for GLP-1 and exendin-4 are lower than those reported in ref *34*. Apart from the different methods used (filter assays in ref *34*; surface plasmon resonance spectroscopy in our study), the lower affinities reported here might result from the presence of Brij micelles as part of the refolding assay established for the full-length GLP-1R.

In conclusion, we show that the established protocols lead to a correctly folded, functional full-length GLP-1R and might be applicable for other proteins of this class. The application of the surface plasmon resonance technique permitted monitoring of the receptor−ligand interaction in real time and can be used for the screening for novel ligands of GPCRs. The in vitro refolded GLP-1R (or appropriate variants thereof) can now be subjected to crystallization trials or solid-state NMR spectroscopic analysis to gather the desired structural information for GLP-1R in the near future.

ACKNOWLEDGMENT

We gratefully thank Uta Best for technical assistance during expression of the constructs in a bioreactor and Dr. Angelika Schierhorn for analysis of peptide masses. We thank Novo Nordisk for supplying high-quality peptides.

SUPPORTING INFORMATION AVAILABLE

Fluorescence emission spectra of the refolded and denatured GLP-1R, RP-HPLC chromatogram of the nGLP-1R, and ligand binding analysis of the nGLP-1R by surface plasmon resonance. This material is available free of charge via the Internet at http://pubs.acs.org.

REFERENCES

1. Thorens, B. (1992) Expression Cloning of the Pancreatic β-Cell Receptor for the Gluco-Incretin Hormone Glucagon-Like Peptide-1. *Proc. Natl. Acad. Sci. U.S.A. 89*, 8641–8645.
2. Fredriksson, R., Lagerstrom, M. C., Lundin, L. G., and Schioth, H. B. (2003) The G-protein-coupled receptors in the human genome form five main families. Phylogenetic analysis, paralogon groups, and fingerprints. *Mol. Pharmacol. 63*, 1256–1272.
3. Cao, Y. J., Gimpl, G., and Fahrenholz, F. (1995) The Amino-Terminal Fragment of the Adenylate-Cyclase Activating Polypeptide (Pacap) Receptor Functions as a High-Affinity Pacap Finding Domain. *Biochem. Biophys. Res. Commun. 212*, 673–680.
4. Grauschopf, U., Lilie, H., Honold, K., Wozny, M., Reusch, D., Esswein, A., Schäfer, W., Rücknagel, K. P., and Rudolph, R. (2000) The N-terminal fragment of human parathyroid hormone receptor 1 constitutes a hormone binding domain and reveals a distinct disulfide pattern. *Biochemistry 39*, 8878–8887.
5. Bazarsuren, A., Grauschopf, U., Wozny, M., Reusch, D., Hoffmann, E., Schäfer, W., Panzner, S., and Rudolph, R. (2002) In vitro folding, functional characterization, and disulfide pattern of the extracellular domain of human GLP-1 receptor. *Biophys. Chem. 96*, 305–318.
6. Parthier, C., Kleinschmidt, M., Neumann, P., Rudolph, R., Manhart, S., Schlenzig, D., Fanghanel, J., Rahfeld, J. U., Demuth, H. U., and Stubbs, M. T. (2007) Crystal structure of the incretin-bound extracellular domain of a G protein-coupled receptor. *Proc. Natl. Acad. Sci. U.S.A. 104*, 13942–13947.
7. Perley, M. J., and Kipnis, D. M. (1967) Plasma Insulin Responses to Oral and Intravenous Glucose: Studies in Normal and Diabetic Subjects. *J. Clin. Invest. 46*, 1954–1962.
8. Holst, J. J. (2007) The physiology of glucagon-like peptide 1. *Physiol. Rev. 87*, 1409–1439.
9. Kieffer, T. J., McIntosh, C. H. S., and Pederson, R. A. (1995) Degradation of Glucose-Dependent Insulinotropic Polypeptide and Truncated Glucagon-Like Peptide-1 in-Vitro and in-Vivo by Dipeptidyl Peptidase-Iv. *Endocrinology 136*, 3585–3596.
10. Eng, J., Kleinman, W. A., Singh, L., Singh, G., and Raufman, J. P. (1992) Isolation and Characterization of Exendin-4, an Exendin-3 Analog, from *Heloderma suspectum* Venom: Further Evidence for an Exendin Receptor on Dispersed Acini from Guinea-Pig Pancreas. *J. Biol. Chem. 267*, 7402–7405.
11. Runge, S., Thogersen, H., Madsen, K., Lau, J., and Rudolph, R. (2008) Crystal structure of the ligand-bound glucagon-like peptide-1 receptor extracellular domain. *J. Biol. Chem. 283*, 11340–11347.
12. Underwood, C. R., Garibay, P., Knudsen, L. B., Hastrup, S., Peters, G. H., Rudolph, R., and Reedtz-Runge, S. (2009) Crystal structure of glucagon-like peptide-1 in complex with the extracellular domain of the glucagon-like peptide-1 receptor. *J. Biol. Chem. 285*, 723–730.
13. Grace, C. R. R., Perrin, M. H., Gulyas, J., DiGruccio, M. R., Cantle, J. P., Rivier, J. E., Vale, W. W., and Riek, R. (2007) Structure of the N-terminal domain of a type B1 G protein-coupled receptor in complex with a peptide ligand. *Proc. Natl. Acad. Sci. U.S.A. 104*, 4858–4863.
14. Sun, C. H., Song, D. Y., Davis-Taber, R. A., Barrett, L. W., Scott, V. E., Richardson, P. L., Pereda-Lopez, A., Uchic, M. E., Solomon, L. R., Lake, M. R., Walter, K. A., Hajduk, P. J., and Olejniczak, E. T. (2007) Solution structure and mutational analysis of pituitary adenylate cyclase-activating polypeptide binding to the extracellular domain of PAC1-Rs. *Proc. Natl. Acad. Sci. U.S.A. 104*, 7875–7880.
15. Pioszak, A. A., and Xu, H. E. (2008) Molecular recognition of parathyroid hormone by its G protein-coupled receptor. *Proc. Natl. Acad. Sci. U.S.A. 105*, 5034–5039.
16. Michalke, K., Graviere, M.-E., Huyghe, C., Vincentelli, R., Wagner, R., Pattus, F., Schröder, K., Oschmann, J., Rudolph, R., Cambillau, C., and Desmyter, A. (2009) Mammalian G-protein-coupled receptor expression in *Escherichia coli*: I. High-throughput large-scale production as inclusion bodies. *Anal. Biochem. 386*, 147–155.
17. Sarramegna, V., Demange, P., Milon, A., and Talmont, F. (2002) Optimizing functional versus total expression of the human μ-opioid receptor in Pichia pastoris. *Protein Expression Purif. 24*, 212–220.
18. Rasmussen, S. G. F., Choi, H. J., Rosenbaum, D. M., Kobilka, T. S., Thian, F. S., Edwards, P. C., Burghammer, M., Ratnala, V. R. P., Sanishvili, R., Fischetti, R. F., Schertler, G. F. X., Weis, W. I., and Kobilka, B. K. (2007) Crystal structure of the human β_2 adrenergic G-protein-coupled receptor. *Nature 450*, 383–388.
19. Baneres, J. L., Martin, A., Hullot, P., Girard, J. P., Rossi, J. C., and Parello, J. (2003) Structure-based analysis of GPCR function: Conformational adaptation of both agonist and receptor upon leukotriene B-4 binding to recombinant BLT1. *J. Mol. Biol. 329*, 801–814.
20. Baneres, J. L., Mesnier, D., Martin, A., Joubert, L., Dumuis, A., and Bockaert, J. (2005) Molecular characterization of a purified 5-HT4

receptor: A structural basis for drug efficacy. *J. Biol. Chem. 280*, 20253–20260.
21. Harding, P. J., Attrill, H., Ross, S., Koeppe, J. R., Kapanidis, A. N., and Watts, A. (2007) Neurotensin receptor type 1: *Escherichia coli* expression, purification, characterization and biophysical study. *Biochem. Soc. Trans. 35*, 760–763.
22. Muller, I., Sarramegna, V., Renault, M., Lafaquiere, V., Sebai, S., Milon, A., and Talmont, F. (2008) The full-length μ-opioid receptor: A conformational study by circular dichroism in trifluoroethanol and membrane-mimetic environments. *J. Membr. Biol. 223*, 49–57.
23. Palczewski, K., Kumasaka, T., Hori, T., Behnke, C. A., Motoshima, H., Fox, B. A., Le Trong, I., Teller, D. C., Okada, T., Stenkamp, R. E., Yamamoto, M., and Miyano, M. (2000) Crystal structure of rhodopsin: A G protein-coupled receptor. *Science 289*, 739–745.
24. Warne, T., Serrano-Vega, M. J., Baker, J. G., Moukhametzianov, R., Edwards, P. C., Henderson, R., Leslie, A. G. W., Tate, C. G., and Schertler, G. F. X. (2008) Structure of a β_1-adrenergic G-protein-coupled receptor. *Nature 454*, 486–491.
25. Jaakola, V. P., Griffith, M. T., Hanson, M. A., Cherezov, V., Chien, E. Y. T., Lane, J. R., IJzerman, A. P., and Stevens, R. C. (2008) The 2.6 Angstrom Crystal Structure of a Human A_{2A} Adenosine Receptor Bound to an Antagonist. *Science 322*, 1211–1217.
26. Rozema, D., and Gellman, S. H. (1995) Artificial Chaperones: Protein Refolding Via Sequential Use of Detergent and Cyclodextrin. *J. Am. Chem. Soc. 117*, 2373–2374.
27. Runge, S., Schimmer, S., Oschmann, J., Schiodt, C. B., Knudsen, S. M., Jeppesen, C. B., Madsen, K., Lau, J., Thogersen, H., and Rudolph, R. (2007) Differential structural properties of GLP-1 and exendin-4 determine their relative affinity for the GLP-1 receptor N-terminal extracellular domain. *Biochemistry 46*, 5830–5840.
28. Rudolph, R., Böhm, G., Lilie, H., and Jaenicke, R. (1997) in Protein Function: A Practical Approach (Creighton, T. E., Ed.) pp 57−96, Oxford University Press, New York.
29. Schmid, F. X. (1997) Optical spectroscopy to characterize protein conformation and conformational changes. In Protein Structure: A Practical Approach (Creighton, T. E., Ed.) pp 261−297, Oxford University Press, New York.
30. Böhm, G., Muhr, R., and Jaenicke, R. (1992) Quantitative Analysis of Protein Far UV Circular Dichroism Spectra by Neural Networks. *Protein Eng. 5*, 191–195.
31. Patterson, S. D., and Katta, V. (1994) Prompt Fragmentation of Disulfide-Linked Peptides during Matrix-Assisted Laser-Desorption Ionization Mass-Spectrometry. *Anal. Chem. 66*, 3727–3732.
32. Kalkhof, S., Haehn, S., Ihling, C., Paulsson, M., Smyth, N., and Sinz, A. (2008) Determination of disulfide bond patterns in laminin β1 chain N-terminal domains by nano-high-performance liquid chromatography/matrix-assisted laser desorption/ionization time-of-flight/time-of-flight mass spectrometry. *Rapid Commun. Mass Spectrom. 22*, 1933–1940.
33. de Maturana, R. L., and Donnelly, D. (2002) The glucagon-like peptide-1 receptor binding site for the N-terminus of GLP-1 requires polarity at Asp198 rather than negative charge. *FEBS Lett. 530*, 244–248.
34. de Maturana, R. L., Willshaw, A., Kuntzsch, A., Rudolph, R., and Donnelly, D. (2003) The isolated N-terminal domain of the glucagon-like peptide-1 (GLP-1) receptor binds exendin peptides with much higher affinity than GLP-1. *J. Biol. Chem. 278*, 10195–10200.
35. Civjan, N. R., Bayburt, T. H., Schuler, M. A., and Sligar, S. G. (2003) Direct solubilization of heterologously expressed membrane proteins by incorporation into nanoscale lipid bilayers. *BioTechniques 35*, 556–560.
36. Buchner, J., and Rudolph, R. (1991) Renaturation, Purification and Characterization of Recombinant Fab-Fragments Produced in *Escherichia coli*. *Nat. Biotechnol. 9*, 157–162.
37. Gromada, J., Rorsman, P., Dissing, S., and Wulff, B. S. (1995) Stimulation of Cloned Human Glucagon-like Peptide-1 Receptor Expressed in Hek-293 Cells Induces cAMP-Dependent Activation of Calcium-Induced Calcium Release. *FEBS Lett. 373*, 182–186.
38. Kieffer, T. J., Heller, R. S., Unson, C. G., Weir, G. C., and Habener, J. F. (1996) Distribution of glucagon receptors on hormone-specific endocrine cells of rat pancreatic islets. *Endocrinology 137*, 5119–5125.
39. Kamitani, S., and Sakata, T. (2001) Glycosylation of human CRLR at Asn123 is required for ligand binding and signaling. *Biochim. Biophys. Acta 1539*, 131–139.
40. Brown, P. J., and Schonbrunn, A. (1993) Affinity Purification of a Somatostatin Receptor-G-Protein Complex Demonstrates Specificity in Receptor-G-Protein Coupling. *J. Biol. Chem. 268*, 6668–6676.
41. Lelianova, V. G., Davletov, B. A., Sterling, A., Rahman, M. A., Grishin, E. V., Totty, N. F., and Ushkaryov, Y. A. (1997) α-Latrotoxin receptor, latrophilin, is a novel member of the secretin family of G protein-coupled receptors. *J. Biol. Chem. 272*, 21504–21508.